ACS OMEGA

http://pubs.acs.org/journal/acsodf

Article

Developmental Toxicity of Surface-Modified Gold Nanorods in the Zebrafish Model

Zain Zaki Zakaria, Nouf N. Mahmoud, Fatiha M. Benslimane, Huseyin C. Yalcin, Ala-Eddin Al Moustafa, and Maha Al-Asmakh*

Cite This: https://doi.org/10.1021/acsomega.2c01313

Read Online

ACCESS | Metrics & More | Article Recommendations

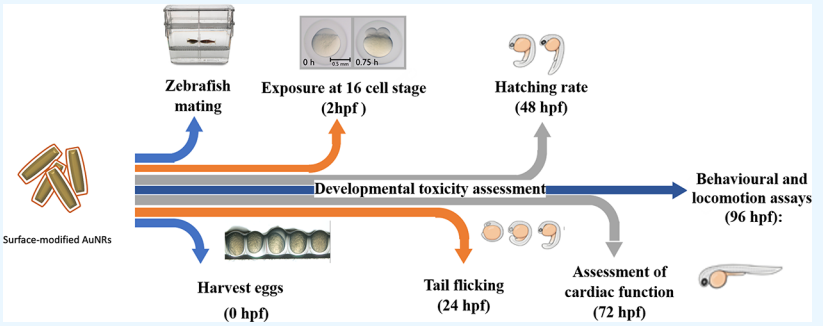

ABSTRACT: Background: nanotechnology is one of the fastest-growing areas, and it is expected to have a substantial economic and social impact in the upcoming years. Gold particles (AuNPs) offer an opportunity for wide-ranging applications in diverse fields such as biomedicine, catalysis, and electronics, making them the focus of great attention and in parallel necessitating a thorough evaluation of their risk for humans and ecosystems. Accordingly, this study aims to evaluate the acute and developmental toxicity of surface-modified gold nanorods (AuNRs), on zebrafish (*Danio rerio*) early life stages. Methods: in this study, zebrafish embryos were exposed to surface-modified AuNRs at concentrations ranging from 1 to 20 μg/mL. Lethality and developmental endpoints such as hatching, tail flicking, and developmental delays were assessed until 96 h post-fertilization (hpf). Results: we found that AuNR treatment decreases the survival rate in embryos in a dose-dependent manner. Our data showed that AuNRs caused mortality with a calculated LC50 of $EC_{50,24hpf}$ of AuNRs being 9.1 μg/mL, while a higher concentration of AuNRs was revealed to elicit developmental abnormalities. Moreover, exposure to high concentrations of the nanorods significantly decreased locomotion compared to untreated embryos and caused a decrease in all tested parameters for cardiac output and blood flow analyses, leading to significantly elevated expression levels of cardiac failure markers *ANP/NPPA* and *BNP/NPPB*. Conclusions: our results revealed that AuNR treatment at the EC_{50} induces apoptosis significantly through the *P53*, *BAX/BCL-2*, and *CASPASE* pathways as a suggested mechanism of action and toxicity modality.

1. INTRODUCTION

The nanotechnology revolution provides a wide range of applications in biomedical industries, engineering, agriculture, electronics, energy, and other fields.[1] Consequently, the production of various nanomaterials is advancing rapidly to match industrial and research purposes, raising the nanotechnology market worldwide. However, careful evaluation of the toxicological and hazardous aspects of nanomaterials and their underlying molecular mechanisms is crucial to ensure human and environmental safety and maintain sustainable production of nanomaterials.[2]

Although mammals, including rodents, are the most commonly used animal models to evaluate the biological and toxicity profiles of chemicals and nanomaterials; however, these models cannot meet the high demand of toxicity screening for various emerging nanomaterials.[3] The zebrafish (*Danio rerio*) is a prominent model widely used to evaluate various biological and toxicological responses.[4] This model has several unique merits over mammalian models in several aspects; its small size and the rapid development of embryos enable cost-effective replicates to be conducted.[3,5] Besides, the zebrafish model provides an in-depth understanding of the underlying mechanisms of toxicity since zebrafish and humans share significant physiological and anatomical similarities.[2] Moreover, using this model, real-time and non-invasive tracking of drugs'

Received: March 4, 2022
Accepted: August 2, 2022

Figure 1. Embryonic phenotypes for high concentration treatment of AuNRs. Images of 72 hpf embryos were examined under a light microscope (30× magnification). (A) Control embryos show normal development without malformations. (B) 10 μg/mL treated embryos show abnormal development with pericardial edema, yolk sac edema, and lordosis.

bio-distribution is possible.[6] The zebrafish model is valuable for nanoparticle studies due to the ease of nanoparticle exposure without the need for injection.[7]

Several studies regarding drug delivery, toxicity, and bio-distribution of nanomaterials have been conducted in the literature using the zebrafish model. Such studies have been made to assess the toxicity of silver and copper nanoparticles[8] and the inflammation-coagulation response caused by silica nanoparticles.[9] In addition, a recent study by Hu *et al.* pointed out that polystyrene nanoparticles activated the p38 MAPK pathway and induced apoptosis in zebrafish and macrophage cells.[10]

Gold nanoparticles (AuNPs) have several applications in imaging, diagnosis, therapy, and drug delivery among nanomaterials due to their unique physical and plasmonic properties.[11] The zebrafish model was used in several studies to predict the toxicity of AuNPs; however, the majority of investigations focused so far on its spherical shape type. Nevertheless, several reports indicate that the toxicity of AuNPs is correlated with nanoparticles' shape, size, and surface chemistry;[12] for example, recent research suggested that the uptake amount of AuNPs and their toxicity in zebrafish was significant for large particles of AuNPs compared to their smaller counterparts.[13] Moreover, Kim *et al.* found that AuNP coated with *N,N,N*-trimethylammoniumethanethiol affected eye development and caused neuronal damage in the developing zebrafish.[14] The surface functionalization of nanoparticles significantly impacts their colloidal stability, toxicity, and cellular and tissue internalization.[15] Ligand exchange using thiolated moieties is considered one of the most widely utilized strategies to remove the surfactants (such as cetrimonium bromide) from the nanorods' surface, consequently eliminating their biological toxicity.[16]

In our previous work, rod-shaped AuNP functionalized with polyethylene glycol (PEG)-phospholipid ligand demonstrated enhanced colloidal stability and increased transdermal delivery properties.[17] Furthermore, they exhibited high cytotoxicity against a panel of breast cancer cell lines[18] and demonstrated anti-angiogenesis properties.[19] We demonstrated in our previous work that AuNRs conjugated with a phospholipid moiety modulated several apoptotic signaling pathways in breast cancer cells through activation of TNF and *p53* signaling pathways, and other regulatory genes contributed to proapoptotic pathways and by suppression of antiapoptotic pathways.[20] In this study, we explored the toxicity of gold nanorods (AuNRs) modified with a phospholipid moiety on the normal embryonic development of zebrafish using organ-specific toxicity assays (cardiotoxicity and neurotoxicity) and apoptotic markers to further understand their mechanism of action and toxicity modality.

2. RESULTS

2.1. Synthesis and Characterization of AuNRs. AuNRs were successfully synthesized, functionalized with phospholipid, and characterized, as described previously.[19] UV−vis spectrophotometry demonstrated the typical longitudinal and transverse peaks of the golden nanorods (GNRs) at ∼523 nm and 760 nm, respectively, which suggest their excellent stability. The surface of nanorods was functionalized with a phospholipid moiety through S−Au linkage to eliminate the toxicity of cetyltrimethylammonium bromide (CTAB) and increase the colloidal stability of the nanorods. The nanorods demonstrated an average hydrodynamic size of ∼78 nm and surface charge of +25 mV before surface functionalization due to the adsorption of CTAB molecules onto the surface of nanorods. The phospholipid-functionalized-GNR demonstrated an average hydrodynamic size of ∼84 nm and effective surface charges of −12 mV. Fourier transform infrared (FTIR) spectroscopy confirmed the surface conjugation with the PEG-DSPE-SH ligand where fading of the S−H small stretching band in the spectrum of phospholipid-PEG-GNRs supported the successful binding of the DSPE-PEG-SH ligand to the surface of GNRs.[17,20]

2.2. AuNR Quantification and Cellular Uptake into Zebrafish Embryos by ICP−OES. To quantify the accumulation of thiolated-PEGylated-phospholipid AuNRs in zebrafish embryos, gold concentrations in AuNRs in zebrafish embryos after AuNR treatment were evaluated using inductively coupled plasma-optical emission spectroscopy (ICP−OES Optima DV, PerkinElmer, USA). We treated 50 embryos with 20 μg/mL AuNRs, the ICP−OES mass reading in our sample was (1759.6 ng/g), indicating that the internalized gold into the zebrafish sample (50 embryos—0.26 g dry) after 6 h of incubation was 457.5 ng. The findings show that a significant quantity of the nanorods were internalized into zebrafish embryo cells, which amplified their effect after 6 h of incubation and finally led to cellular apoptosis and death. Nanoparticles' cellular absorption is critical for their biological reactions and toxicity; nanoparticles have been coupled with particular ligands to increase their internalization and, hence, activity. According to a recent study, the PEG-GNP, a virtually neutral GNP, had a considerable impact on developing zebrafish. As a result of this study,

https://doi.org/10.1021/acsomega.2c01313
ACS Omega XXXX, XXX, XXX−XXX

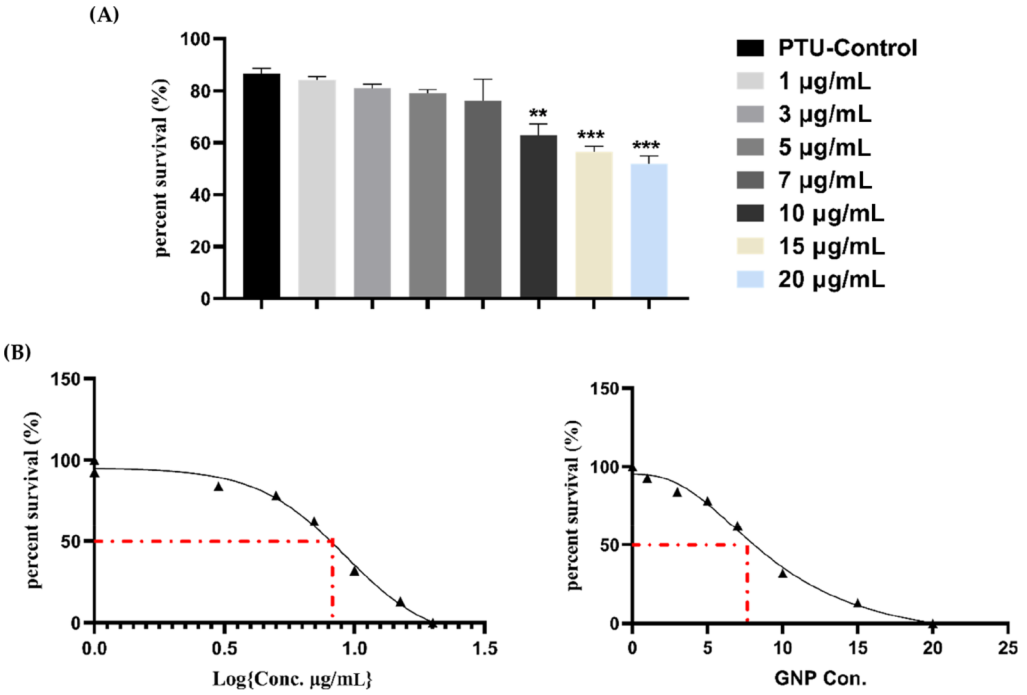

Figure 2. (A) Survival rate of embryos at 24 h post-fertilization. (B) Effective response curve of embryos exposed to AuNRs. The hypothetical EC50 was calculated using Graph pad software to be 9.163 μg/mL. All data are presented as mean ± SEM (20 embryos were used in each group; the experiment was performed in triplicate). One-way ANOVA with the Sidak post hoc test was used to compare the differences between groups. *p < 0.05, **p < 0.01, ***p < 0.001, and ****p < 0.0001.

questions about the safety of PEGylated gold nanoparticle use in medicine and nano-biotechnology have been raised.[21]

2.3. Developmental Toxicity. Malformations were only occasionally observed at a low concentration of AuNRs; however, the malformation rate significantly increased compared to controls at high concentrations. The most commonly observed malformations were pericardial edema and yolk sac edema. Other malformations observed at high concentrations were malformed jaw, lordosis, kinked tail, and abnormal body axis curvature (Figure 1).

2.3.1. Survival Rate (24 hpf). At 24 h post-fertilization, the survival rate of embryos was calculated by dividing the number of alive embryos by the total number X100. Embryos were assessed for survival and morphological changes every 24 h until the end of the experiment at 5 dpf. As shown in (Figure 2a), the survival rate was assessed at 24 hpf. There were no significant differences in the mean survival rate between the low concentration groups (1, 3, 5, and 7 μg/mL) and the control group. The survival rate decreased as the concentrations of AuNR increased; this increase was significant between treated embryos with high concentrations (10, 15, and 20 μg/mL) and controls. At 10 μg/mL AuNRs a 20% increase in mortality was observed ($p < 10^{-2}$), while at 15and 20 μg/mL, a 30% increase ($p < 10^{-3}$) was noted. The hypothetical EC50 for the golden nanoparticles according to the 24 hpf sigmoidal curve was calculated to be 9.163 μg/mL (Figure 2b); this was expected as all the phenotypes started to appear at concentrations ≥10 μg/mL.

2.3.2. Hatching Rate (48 hpf). To investigate the impact of AuNRs on the neuromuscular system, we analyzed phenotypes that showed neural and muscle cell development, including tail flicking and hatching function. The hatching rate is the number of hatched embryos from their chorion, divided by the total of survived embryos at 48 h post-fertilization. Our data showed that AuNR treatment is associated with increased embryo hatching. As shown in Figure 3, the hatching percentage was

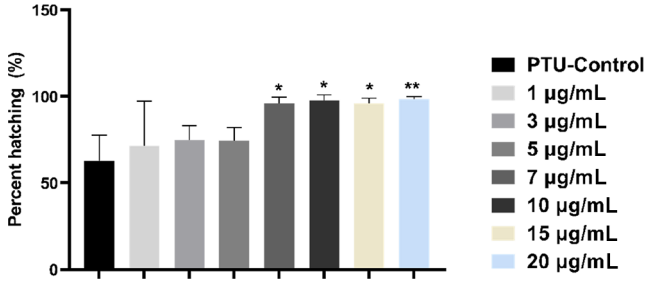

Figure 3. Effect of AuNRs on the hatching of zebrafish embryos at 48 hpf. All data are presented as mean ± SEM (20 embryos were used in each group; the experiment was performed in triplicate). One-way ANOVA with the Sidak post hoc test was used to compare the differences between groups. *p < 0.05, **p < 0.01, ***p < 0.001, and ****p < 0.0001.

increased by 1.5-fold ($p < 10^{-4}$) at 48 hpf; starting from 7 μg/mL nanoparticles concentration up to 15 μg/mL, there was a significant increase in the hatching rate.

2.3.3. Tail Flicking Assay (24 hpf). For the tail flicking test, the number of tail flicking of embryos inside their chorions at 24 h post-fertilization is counted for 10 s and multiplied by 6 to complete a minute. As shown in Figure 4, at high concentrations of AuNRs (15 and 20 μg/mL), tail flicking increased by 1.3-fold ($p < 10^{-1}$) at 24 hpf, indicating a potential effect on the neuromuscular system.

2.4. Behavioral and Locomotion Assay (96 hpf). We performed a locomotion assay to further support the tail flicking data, where AuNR-treated embryos were exposed to alternating light/dark episodes. In most cases, the affected or intoxicated

https://doi.org/10.1021/acsomega.2c01313
ACS Omega XXXX, XXX, XXX−XXX

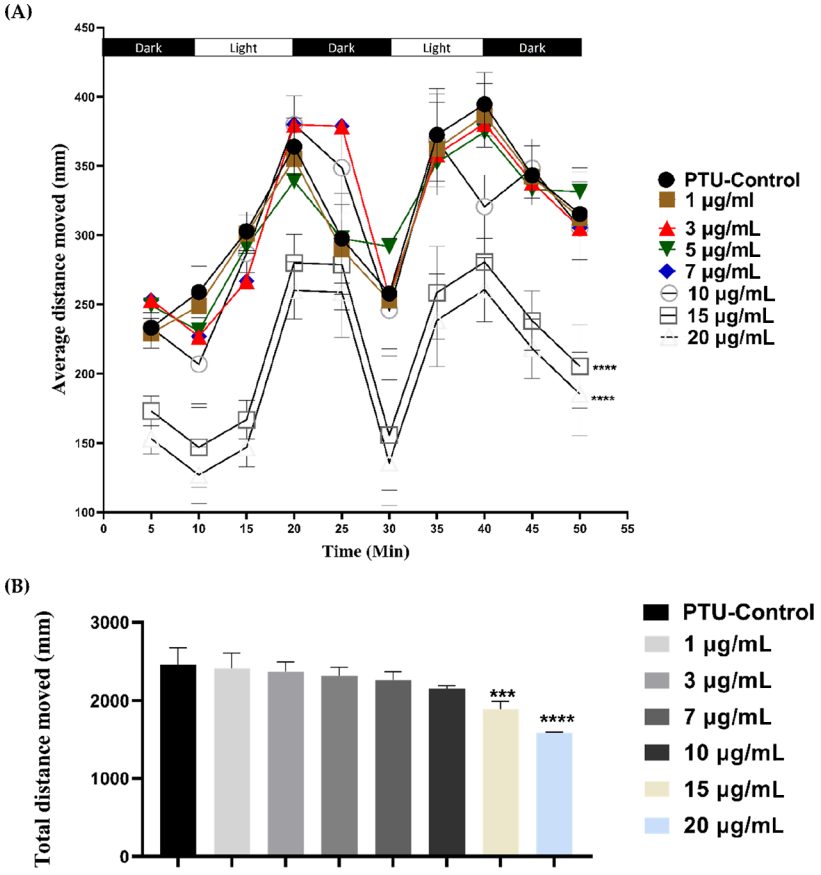

Figure 4. Assessment of the potential effect of AuNRs on the muscular system in the experimental group at 24 hpf. All data are presented as mean ± SEM (50 embryos were used in each group; the experiment was performed in triplicate). One-way ANOVA with the Sidak post hoc test was used to compare the differences between groups. *$p < 0.05$, **$p < 0.01$, ***$p < 0.001$, and ****$p < 0.0001$.

zebrafish embryos exhibit weak or increased movement when stimulated by light. Behavior and locomotion assay was performed on 96 h post-fertilization for all groups. As shown in Figure 5, the test was performed for 50 min divided by 10 min of light and dark to monitor the zebrafish's response to light and its behavior in both conditions. The behavior was assessed by the distance each embryo traveled in millimeter.

AuNRs at low concentrations (1, 3, 5, and 7 μg/mL) had no effect on the locomotion assay as AuNR-treated zebrafish groups' behavior mimicked those in the control group; their movement increased in the light periods and decreased in the dark. However, at a high concentration of AuNRs (15 and 20 μg/mL), there was a significant decrease by 1.1−1.5 fold ($p < 10^{-4}$) in the average distance moved and total distance moved, as shown in Figure 5A,B, respectively.

2.5. Cardiac Toxicity: Assessment of the Cardiac Function. *2.5.1. Live Imaging of Zebrafish (72 hpf).* To assess the effect of AuNR treatment on zebrafish embryos' cardiovascular system, cardiac function parameter measurements were performed on the two main blood vessels of the zebrafish dorsal aorta (DA) and posterior cardinal vein (PCV). Cardiac output (CO) and blood flow analyses for DA and PCV showed approximately the same trend. A decrease in all tested parameters among all experimental groups is associated with increase in the AuNR concentration. There was no significant difference in any tested parameter between the controls and low concentrations of AuNR (1, 3, 5, 7, and 10 μg/mL)-treated embryos (Figure 6). The significant decrease in DA diameter, as well as blood velocity, was apparent at the highest two concentrations of AuNR-treated groups (15 and 20 μg/mL), which in turn significantly reduced the overall CO by 1−1.2-fold ($p < 10^{-4}$). Collectively, our data suggested that a high concentration of AuNRs might affect cardiomyogenesis during zebrafish development.

2.6. Cardiac Failure Biomarker Expression (72 hpf). To further explore the effect of AuNRs on cardiac functions at the molecular level, we investigated the expression of cardiac failure markers *ANP/NPPA* and *BNP/NPPB* in all experimental groups at 72 h post-fertilization. Our findings suggest that AuNRs at high concentrations (10, 15, and 20 μg/mL) lead to a significant increase in the expression of *ANP/NPPA* and *BNP/NPPB* by 50% ($p < 10^{-2}$), as shown in Figure 7. The increase in *BNP/NPPB* levels at 72 hpf might slow down the progress of morphological and functional changes in the zebrafish heart, leading to reduced heart rate, shape, and blood velocity.

2.7. Apoptosis Assessment (72 hpf). To investigate whether AuNR treatment would affect apoptosis in zebrafish embryos, staining with acridine orange (AO) was used to determine inappropriate apoptotic cell death. The dye emits green fluorescence when bound to dsDNA and binds particularly strongly to fragmented DNA, resulting from the apoptosis machinery at work. Thus, selective labeling of cells undergoing apoptosis is achieved. AuNR treatment induced several abnormalities and malformation in the zebrafish embryos, including pericardial and yolk sac edemas, as well as malformed Jaw, lordosis, in a dose-dependent manner (Figures 8A & 1). Furthermore, there was a steady increase in the number

https://doi.org/10.1021/acsomega.2c01313
ACS Omega XXXX, XXX, XXX−XXX

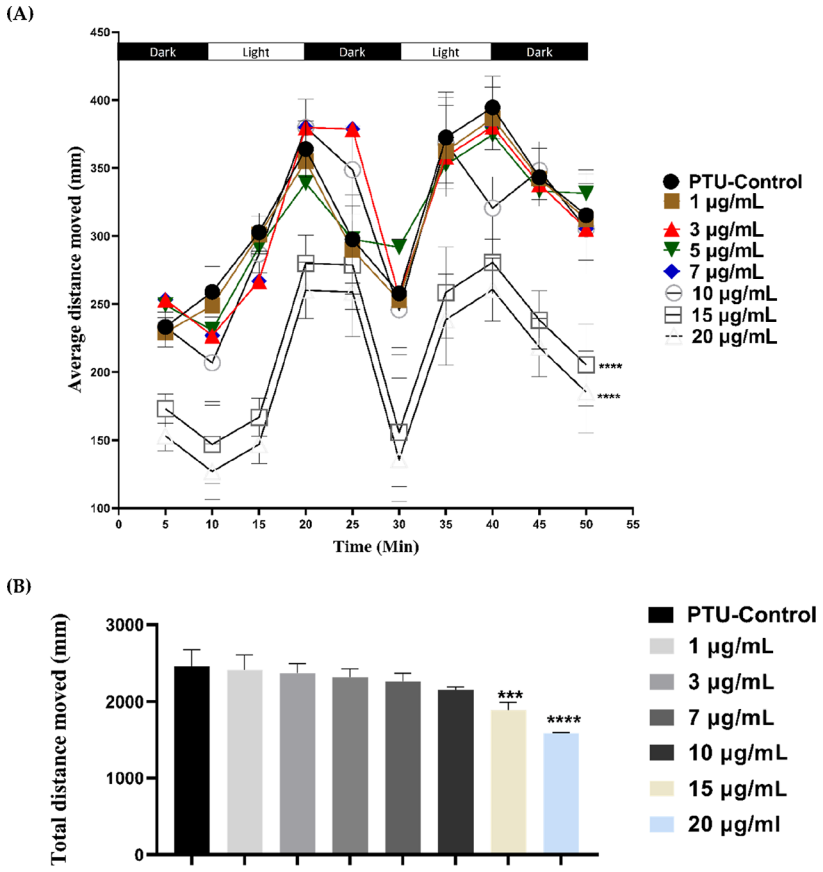

Figure 5. Behavior and locomotion assays of the experimental group at 96 h post-fertilization. (A) Average distance moved (determined using the ViewPoint Microlab system) during every 5 min period by the 96 hpf-old embryos. (B) Total distance moved in millimeter. Data of the locomotion test are presented as mean ± SEM. One-way ANOVA followed by the Dunnett test was used to compare the groups. *$p < 0.05$, **$p < 0.01$, ***$p < 0.001$, and ****$p < 0.0001$, $n = 20$.

of apoptotic cells with the increase in the AuNR concentration in a dose-dependent manner.

The dose-dependent effects of AuNRs were quantitated using a fluorescence microplate reader (Figure 8B). This is a primary screening method to identify agents that modulate apoptosis in entire embryos. Our results showed that apoptosis significantly appeared at (10 μg/mL) of AuNRs. The highest AuNR concentration (20 μg/mL) was associated with a 5.3-fold increase in apoptosis ($p < 10^{-4}$).

2.8. AuNRs Induces Cytotoxicity of Zebrafish Embryos through Intrinsic Apoptosis Pathways. The expression patterns of genes implicated in apoptosis (*P53*, *BAX/ZBAX1*, *BCL2/ZBLP2*, *CASPASE 3/ZCASPASE-3*, and *CASPASE 8/ZCASPASE-8*) were explored in zebrafish embryos treated with 1, 3, 5, 7,10, 15, and 20 μg/mL of AuNRs and then compared to untreated controls (only PTU). The results revealed that the expression level of *p*53, a gene that has ability to activate apoptosis,[22,23] was significantly upregulated in treated groups at a high concentration of AuNRs (10 and 15 μg/mL with a *p*-value of <0.01 and 20 μg/mL with *p*-value of <0.001, Figure 9). A similar pattern was also seen in the expression of *BAX/ZBAX1*, which was dramatically increased in those treated with high concentrations of AuNRs (10 and 15 μg/mL with a *p*-value of <0.01 and 20 μg/mL with a *p*-value of <0.001). *BAX/ZBAX1* has been shown to be involved in *p53*-mediated apoptosis.[24] On the other hand, BCL2 family of proteins is one of the most important regulators of apoptosis.[25] In the groups treated with high concentrations of AuNRs, the *BCL2* gene expression level was significantly downregulated at concentrations 15 and 20 μg/mL ($p < 0.01$); however, the gene expression was not significantly affected at lower concentrations of AuNRs.

As for the *CASPASE 3* and *CASPASE 8* which are also involved in apoptosis,[26] both caspases were significantly upregulated in the highest concentration of AuNR-treated groups (15 and 20 μg/mL with *p*-value of <0.01 and $p < 0.001$, respectively).

3. DISCUSSION

AuNPs and particularly non-spherical types such as AuNRs are frequently utilized in several biomedical applications due to their unique features related to their particle size, surface chemistry, and plasmonic properties.[27] AuNP surface modification modulates their biological responses such as cytotoxicity, cellular uptake, bio-distribution, and cellular death modalities.[28]

In this study, AuNRs were successfully synthesized using a binary surfactant system and functionalized with a thiolated-PEGylated-phospholipid moiety. The presence of PEG has enhanced the colloidal stability of the functionalized nanorods upon exposure to biological media. The surface modification has occurred through surface ligand exchange due to the high affinity of gold toward thiolated ligands.[29] This surface functionalization of AuNRs enhances their colloidal stability in biological media and reduces the concentration of CTAB, a toxic surfactant involved in the synthesis of AuNRs.[30]

AuNRs have a great interest in biomedical applications including imaging, diagnosis, and therapy. However, their

https://doi.org/10.1021/acsomega.2c01313
ACS Omega XXXX, XXX, XXX−XXX

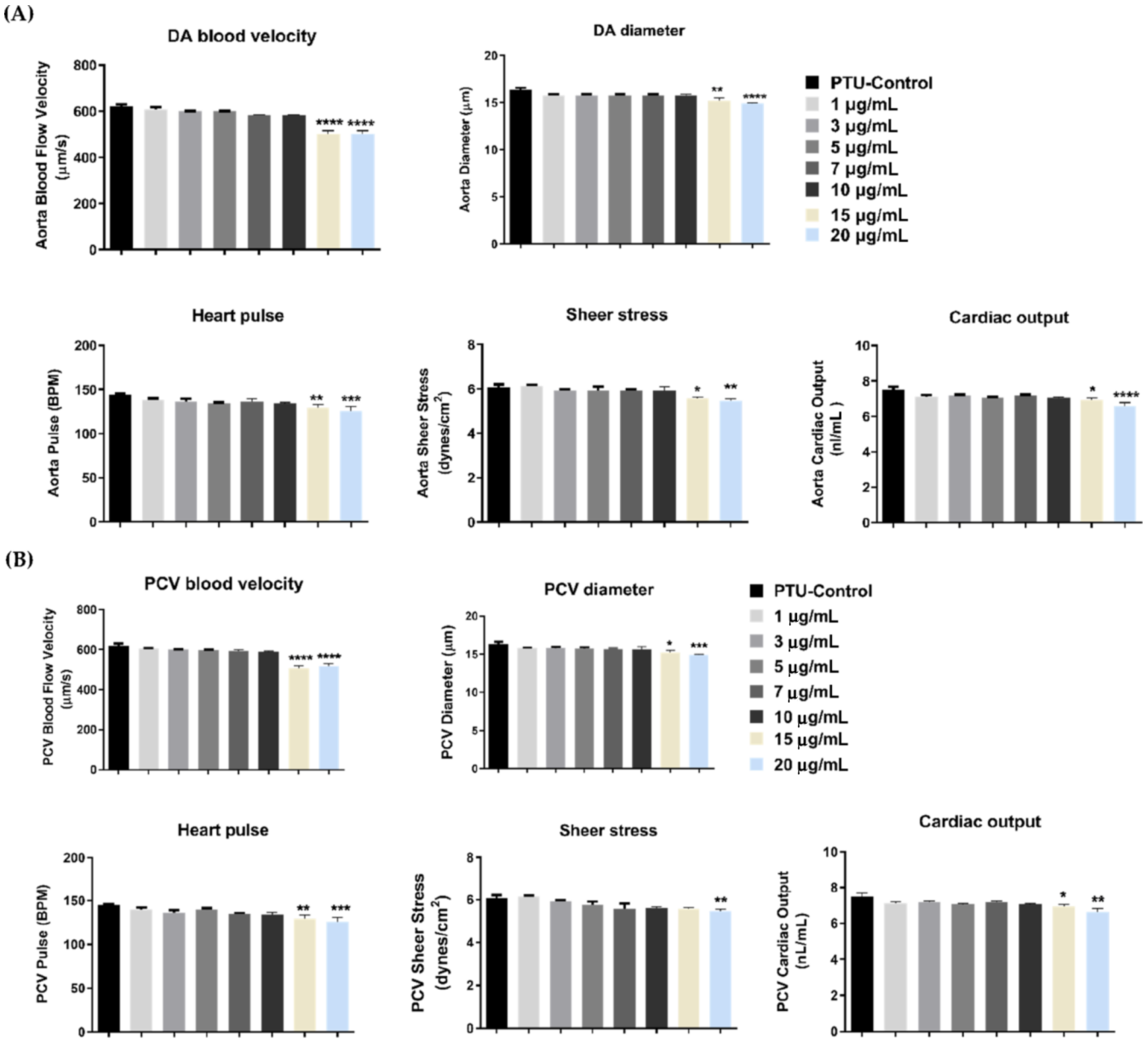

Figure 6. Assessment of the cardiac function of the experimental group at 72 h post-fertilization (A) DA and (B) PCV blood flow analysis. All data are presented as mean ± SEM (six embryos were used in each group; the experiment was performed in triplicate). One-way ANOVA with the Sidak post hoc test was used to compare the groups. *$p < 0.05$, **$p < 0.01$, ***$p < 0.001$, and ****$p < 0.0001$.

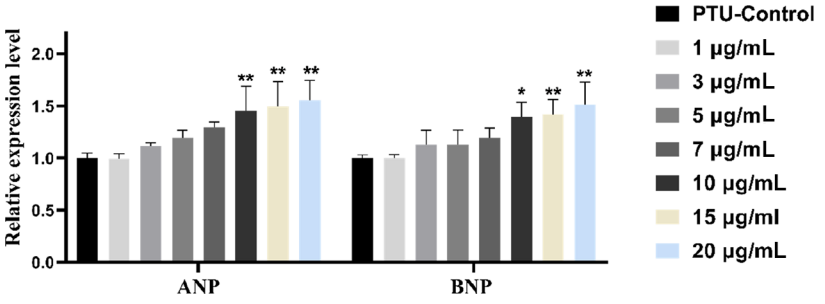

Figure 7. Cardiac failure biomarkers expression of experimental groups at 72 h post-fertilization. All data are presented as mean ± SEM (experiments were carried out in triplicate). One-way ANOVA followed by the Dunnett test was used to compare the groups. *$p < 0.05$, **$p < 0.01$, ***$p < 0.001$, and ****$p < 0.0001$.

toxicity aspects are not thoroughly investigated. Our previous reports demonstrated the cytotoxicity effect of AuNRs decorated with phospholipid against a panel of breast cancer cells and their antiangiogenic activity using the chicken embryo

https://doi.org/10.1021/acsomega.2c01313
ACS Omega XXXX, XXX, XXX−XXX

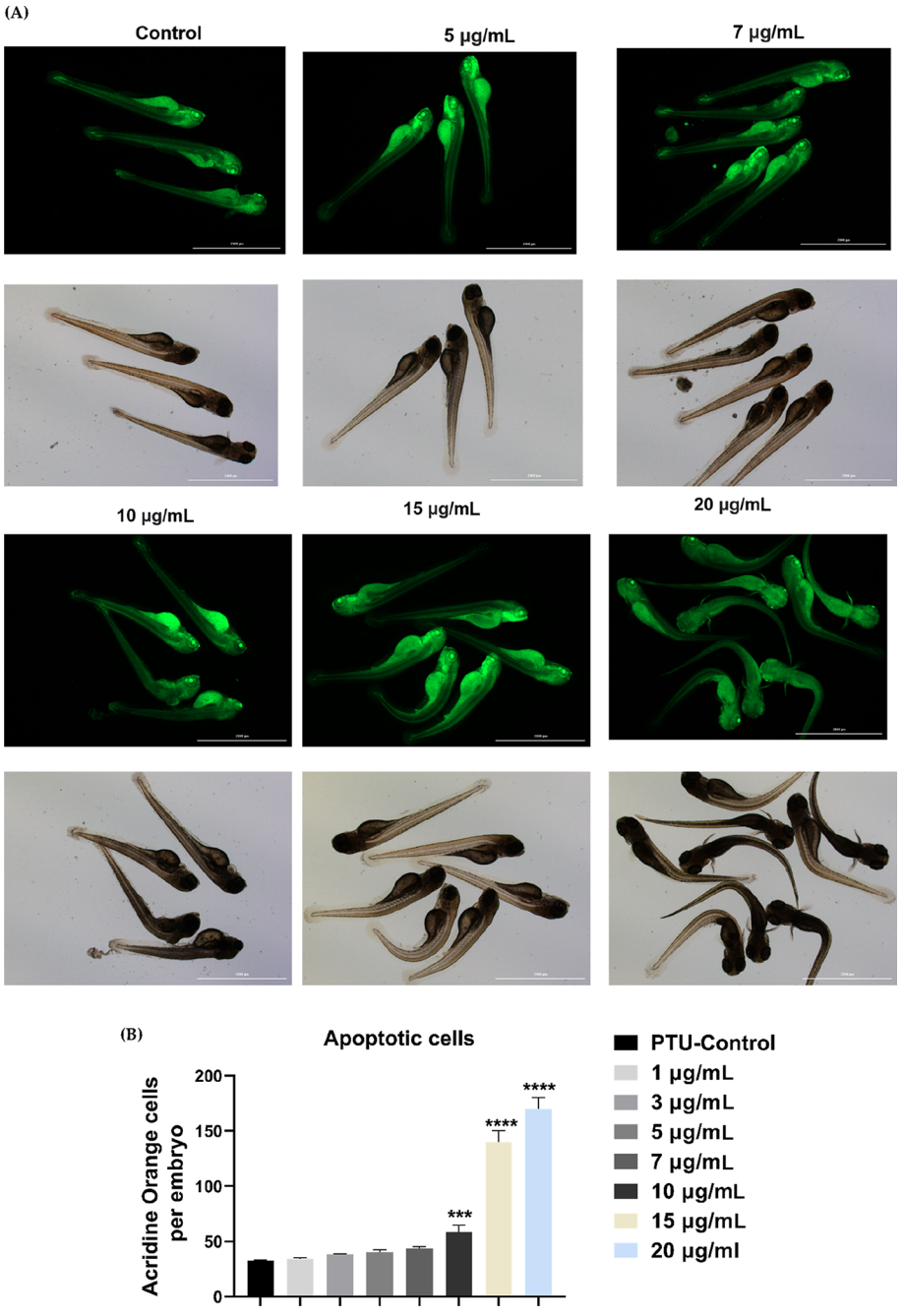

Figure 8. Quantitative analysis for apoptotic cells using AO. AO staining was performed in all experimental groups. (A) Visible morphological changes for all experimental groups. (B) Quantitative analysis using a microplate assay to count the number of green AO positive cells per embryo. All data are presented as mean ± SEM (experiments were carried out in triplicate). One-way ANOVA with the Sidak post hoc test was used to compare the groups. *$p < 0.05$, **$p < 0.01$, ***$p < 0.001$, and ****$p < 0.0001$.

model.[18,19] Herein, we used the zebrafish embryos to provide insights into the impact of these AuNRs on the early stage of embryogenesis and their possible toxicity on the developing body systems, particularly the cardiac and neuromuscular systems.

Different doses of AuNRs (1, 3, 5, 7, 10, 15, and 20 μg/mL) were shown to have a toxic effect on zebrafish embryos throughout the early stages of development. As the concentrations of AuNRs rise, survival rates fall, but there is no discernible difference in survival rates between the low concentration groups and the control. According to the 24 hpf sigmoidal curve, the nanorods' potential EC50 was 9.163 g/mL, in agreement with our data, which showed that all phenotypes appeared at 10 g/mL and higher concentrations. The effects of CTAB-AuNRs on the development of zebrafish embryos exhibited an "all-or-nothing" response as only embryos exposed to the highest concentration showed developmental anomalies, including pericardial edema, yolk sac edema, and tail deformities, as well as malformed Jaw, lordosis, which were noted in a dose-dependent manner.[31] In this frame, many animal species (mice, rats, fruit flies, zebrafish, and filler feeding crustaceans) were tested for AuNP toxicity, that resulted in reduced life span, weight loss, and other detrimental phenotypic and biological outcomes.[32]

https://doi.org/10.1021/acsomega.2c01313
ACS Omega XXXX, XXX, XXX−XXX

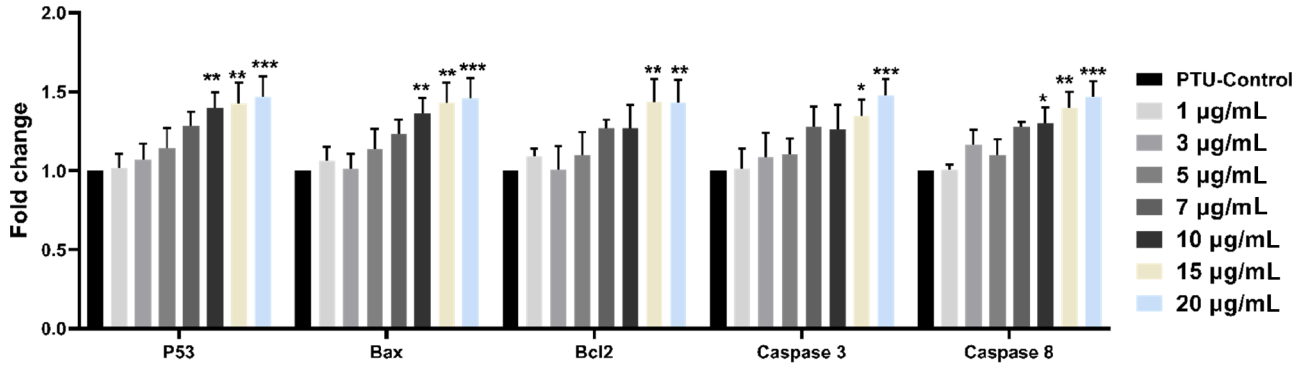

Figure 9. RT-PCR analysis of genes implicated in apoptosis, using zebrafish embryos treated with 1, 3, 5, 7, 10, 15, and 20 μg/mL of AuNRs, compared to the control (only PTU). Data are represented as mean ± standard deviation (SD). $p^* < 0.05$, $^{**}p < 0.01$, $^{***}p < 0.001$, and $^{****}p < 0.0001$.

AuNPs have been reported to diffuse through the chorionic pore canals and reach the inner cell mass of zebrafish embryos, remaining inside throughout the entire development.[33,34] However, it is also reasonable that the adsorption of AuNRs to the chorion may hamper gas exchange (oxygen supply) and osmoregulation, both essential for the development of zebrafish embryos. In line with our results, Wang *et al.* also observed an "all-or-nothing" effect in zebrafish embryos exposed to sublethal doses of AuNRs, with no visible malformations.[31]

We show that AuNRs are successfully taken up and accumulated in tissues by zebrafish during development. These findings support the action of AuNRs and because of the genetic and physiological similarities between zebrafish and humans, our findings can be simply applied to predict the impact of AuNRs on other species.

An investigation of the locomotion and neuromuscular development of embryos that had been exposed to AuNRs was carried out in order to ascertain the impact these treatments have on embryogenesis and organ development. According to the findings of our study, treatment with AuNRs is associated with enhanced embryo hatching as well as motility and tail coiling, both of which point to a dysfunction in muscle contraction and possible problems in the nervous system. In addition, locomotion assay demonstrated that zebrafish treated with low concentrations of AuNRs exhibited behavior similar to that of those in the control group. On the other hand, treatment with high concentrations of AuNRs resulted in a significant reduction in both the average and total distance traveled. This finding is in agreement with findings from earlier studies, which shows that exposure to high concentrations of AuNRs caused severe malformations.[35]

Collectively, these findings suggested that high concentrations of AuNRs have a negative effect on proper myogenesis in zebrafish embryos, which could result from an impairment of the cellular processes during gastrula and segmentation periods.[36] It is important to indicate that the biological activity of these surface-modified nanorods was observed at concentrations even less than 5 μg/mL.[18]

Meanwhile, adverse effects caused by CTAB-AuNRs were also reported for other organisms. Four cladocerans species have shown reduced body length when exposed to CTAB-AuNRs at concentrations ranging from 1.41 to 18.1 μg/L,[37] whereas white-rot fungi exhibited growth inhibition at concentrations between 15.91 to 33 mg/L of AuNRs−NP-Au.[38] Most of the studies employing zebrafish embryos for toxicity assessment of AuNPs focused on sphere-shaped, and no evident toxicity has been reported. For instance, Browning *et al.* demonstrated that spherical AuNPs (86.2 nm) did not cause significant mortality or malformations at concentrations up to 78 μg/mL.[34] This study showed that AuNRs have a more toxic effect, highlighting that the shape of nanoparticles and the coating material might play a critical role in the AuNR effect. It is worth noting that the concentration of CTAB in our AuNR sample was significantly reduced through surface ligand exchange with the phospholipid moiety and four rounds of centrifugations; thus, the observed toxicity is most likely not related to CTAB.

AuNRs, on the other hand, have been shown to have a deleterious effect on the cardiovascular system of zebrafish embryos that have been exposed to them. Analyses of CO and blood flow demonstrated that high concentrations of AuNRs (15.20 g/mL) have an effect on cardiac functions in comparison to their control embryos. There was no discernible difference, statistically speaking, between the controls and the embryos treated with low concentrations of AuNRs (1, 3, 5, 7, or 10 g/mL) in any of the parameters that were examined. At the highest two doses of AuNRs, the treated groups showed a considerable drop in the diameter of the DA and PCV as well as the velocity of the blood, which led to a significant reduction in the overall CO. The increased expression of *ANP/NPPA* and *BNP/NPPB*, two key heart failure biomarkers, suggests that high concentrations of AuNRs may slow down the progression of morphological and functional development of the zebrafish heart, resulting in decreased heart rate, shape, and blood velocity.[39] Collectively, our data suggest that a high concentration of AuNRs might affect cardio myogenesis during zebrafish development.

Apoptosis is an essential part of development and pathology in vertebrates and is involved in normal cell turnover, eliminating unnecessary cells after differentiation, as well as being activated in response to environmental stress. Moreover, the process of apoptosis during development is very well conserved between zebrafish and higher animals, making the zebrafish a suitable model to study embryotoxic effects under environmental stimuli.[40−42] In this study, the relative fluorescence of larger pools of embryos using digital image analysis was performed. The dose-dependent effects of AuNRs showed that apoptosis significantly appeared at the highest concentrations, which indicate the mechanism of action and the toxicity modality of AuNRs at the cellular level of the developing embryos. Stress-induced apoptosis is thought to be a factor in the pathophysiology of malformations during embryogenesis.[40]

To confirm the results of AO dye and to determine the inappropriate apoptotic cell death, the expression patterns of a set of genes involved in apoptotic pathways including *P53*, *BAX/ZBAX1*, *BCL2/ZBLP2*, *CASPASE 3/ZCASPASE-3*, and *CAS-*

https://doi.org/10.1021/acsomega.2c01313
ACS Omega XXXX, XXX, XXX−XXX

PASE 8/ZCASPASE-8[43] were investigated. We demonstrated that their expression levels in zebrafish exposed to high concentrations of AuNRs reflected a significant difference in apoptotic activity. Moreover, high concentrations of AuNRs upregulated mRNA level of cell cycle checkpoints *P53* and the pro-apoptotic *BAX/zbax1*. Expression of anti-apoptotic gene *BCL2/zBlp2* was downregulated in all treated groups. Furthermore, the expression of the two caspase apoptotic genes *CASPASE 3/ZCASPASE-3* and *CASPASE 8/ZCASPASE-8* increased at higher concentrations of AuNR treatments. In line with these results, AuNRs coated with the phospholipid moiety modulated several signaling pathways involved in cellular apoptosis such as TNF and *p53* pathways and suppressed several genes involved in the anti-apoptotic pathways such as NAIP, BAD, and BFAR.[20] Besides, our previous study revealed that AuNRs decorated with phospholipid exerted significant anti-angiogenesis effect and modulated several apoptotic pathways in the chicken embryo fibroblast model and induced toxicity at the early stage of embryogenesis;[19] such an observed modulation effect on apoptotic pathways in chicken embryo fibroblast cells was detected over a low range of concentration.

It was shown that the molecular machinery behind the intrinsic and extrinsic mechanisms of apoptosis is highly conserved between zebrafish and mammals.[42,44] Upregulation of *p53* results in activation of pro-apoptotic members of the Bcl-2 family, such as *BAX/ZBAX1*, and downregulation of anti-apoptotic genes *BCL2/zBlp2* which causes permeabilization of the outer mitochondrial membrane, allowing soluble proteins from the intermembrane space to enter the cytosol and activate caspases.[22,25,45]

AuNPs penetrate zebrafish eggs through passive diffusion *via* the chorion's pore channels (0.5−0.7 μm in diameter). In a dose-dependent way, the larvae acquire an increasing number of gold nanoparticles,[46] indicating that the concentration gradient of AuNPs in the eggs might be the main mechanism for their passive diffusion in the eggs.[33] Following internalization, AuNPs accumulate in various tissues and organs throughout the embryos and larvae's bodies.[33,34,47]

Once AuNPs have accumulated in various organs, they may interact with biological systems on various levels, potentially causing toxicity to the body.[48] Several toxicological endpoints predicated on possible organ effects, and phenotypical abnormalities are used to assess gold nanoparticle toxicity.

Furthermore, it has been shown that the liver and spleen accumulate the most AuNPs after intravenous injection (24 h up to 2 months),[49,50] indicating that the clearance mechanism of AuNPs is connected to the hepatobiliary system.[50] Thus, nanoparticles are taken up by reticuloendothelial organs (liver and spleen), with the latter having greater filtering effectiveness, as well as both organs having a large number of phagocytic cells and capillary beds.[51]

The oxidative stress induced by AuNPs is thought to be a major contributor to their toxicity.[52] Cellular reactive oxygen species (ROS) levels are closely regulated and maintained in equilibrium. According to previous studies, ROS levels rose in zebrafish embryos treated with AuNPs could induce oxidant damage and inhibit antioxidant progress.[53,54] Moreover, AuNPs induce a considerable increase in apoptotic cell death,[55] and PEG-coated AuNPs cause apoptosis and acute inflammation in mice liver.[56]

Recent studies revealed that the mRNA levels of genes linked to oxidative stress and the apoptotic pathway were elevated in the presence of AuNPs.[48,57] In our study, anti-apoptotic gene BCL-2 was shown to be suppressed by AuNPs, but pro-apoptotic genes *BAX* and *CASPASE-3* were found to be upregulated, and the *BCL2/BAX* ratio decreased, indicating apoptosis. Apoptosis may be induced by Caspase3's ability to cleave various cellular proteins.[58]

According to the increased activity of caspase 8 and 9 which are crucial for maintaining cellular homeostasis in terms of cell division and cell death, cellular apoptosis was induced by exposure to AuNPs. This sort of cell death may be a synergetic impact of mitochondrial dysfunction since it is known that the loss of mitochondrial membrane potential has the ability to enhance or inhibit multiple important regulators of apoptosis.[59] Damage to the mitochondrial function is often accompanied by a considerable increase in ROS and alterations in the redox state (as shown by low levels of glutathione in the intracellular environment).[54]

Taken all together, these findings revealed the importance of oxygen stress and apoptosis in the harmful effects of AuNPs on zebrafish larva and demonstrate that AuNPs may trigger apoptosis through the *P53*, *BAX/BCL-2*, and *CASPASE* pathways.

4. MATERIALS AND METHODS

4.1. Zebrafish Husbandry. AB wild-type zebrafish from the QU zebrafish facility was kept in re-circulating stand-alone aquarium racks from AQUA NEERING ZD560 (San Diego, California, USA) in the Biomedical Research Center- Qatar University. The fish were fed two times daily with a varied diet consisting of hatched brine shrimp (*Artemia sp.*). Adult wild-type zebrafish of the AB strain were raised and kept under standard laboratory conditions, they were bred to generate embryos. In this study, 1−5 dpf were used under ethical approval.[60]

All experiments presented in this paper were conducted under the Qatar University's Institutional Animal Care and Qatar University Institutional Biohazard Committee (QU-IBC) approval.

4.2. Synthesis and Characterization of AuNRs. AuNRs were successfully synthesized, functionalized with PEGylated phospholipid moiety and characterized, as described previously.[19] AuNRs were prepared using a mixture of CTAB (Sigma-Aldrich, USA) and sodium oleate (NaOL, Sigma-Aldrich, USA). Briefly, seed particles were synthesized by adding sodium borohydride ($NaBH_4$, Sigma-Aldrich, USA) to a mixture of CTAB and chloroauric acid ($HAuCl_4$, CTAB, Sigma-Aldrich, USA). The seed solution, silver nitrate, gold salt, and ascorbic acid were added to a growth solution of sodium oleate, CTAB, and silver nitrate (Sigma-Aldrich, USA). Double-round centrifugation of the obtained nanorods was performed for purification, and the nanorod pellets were dispersed in milli-Q water. The concentration of AuNRs was measured by a validated method of ICP−OES at a wavelength of 242.795 nm.

Then, synthesized nanoparticles were functionalized with the PEG-DSPE-SH polymer (Nanosoft polymers, USA) by the addition of 1.0 mg of the ligand to each 1.0 mL twice-centrifuged GNR, the solution was mixed overnight, then centrifuged at 8000 rpm for 8 min. The obtained pellets were collected and stored at 4 °C The nanorods were characterized in terms of optical absorption at 200−1100 nm, ζ potential, and hydrodynamic size using a ζ potential/particle size analyzer, as described previously.[20] The surface functionalization of the nanoparticles was confirmed also by FTIR, as described previously.[17,20]

https://doi.org/10.1021/acsomega.2c01313
ACS Omega XXXX, XXX, XXX−XXX

4.3. Embryo Treatment and AuNR Exposure. The medium used for general handling of the embryos and dilution of all AuNR solutions was N-phenylthiourea 1-phenyl 2-thiourea (PTU; Sigma, St. Louis, MO), which was dissolved in water to 0.2% and diluted in embryo media to the indicated concentrations (0.002 to 0.02%) at specific developmental time points (6 to 22 hpf). PTU treatment alone (control treatment) resulted in embryos that lacked pigment but were otherwise morphologically normal. PTU water is used to suppress pigmentation and make embryos transparent to facilitate taking time-lapse videos.

The desired concentrations of the AuNRs to be tested were determined based on our previous *in vitro* work, and different concentrations were prepared using PTU as the solvent. The embryos were divided into six triplicate groups: control (only PTU) and the seven experimental groups 1, 3, 5, 7, 10, 15, 20 μg/mL of AuNRs. All groups were examined at specific times depending on the experiment running. AuNR exposure continued until 24 hpf, 48 hpf, or 72 hpf.

4.4. Quantification of the Au Uptake by Zebrafish Embryos by ICP−OES. In order to evaluate the uptake of AuNPs in zebrafish embryos using ICP−OES. The following protocol was used: first, at the same developmental stage (4 hpf), viable embryos were harvested and implanted on 24-well plates in embryo media. For 6 hpf at 28 C, embryos were treated with AuNPs diluted in embryo medium 20 μg/mL, as determined in our toxicity assay. The AuNP-treated embryos were collected and washed five times with deionized water. Then, the washed pellets were lyophilized in a vacuum freeze-drier (VirTis SP scientific, USA) for 30 h at 70 °C condensation. Following that, the samples were dissolved in 1 mL of aqua regia (prepared with ICP grade HCl and HNO_3) and digested in Teflon-lined jars under microwave irradiation (MARS-6 microwave digestion equipment, CEM corporation, USA). The resultant solution was diluted to 10 mL with ICP grade water, and the Au content was measured using ICP−OES against a standard calibration curve.

4.5. Developmental Toxicity. Developmental abnormalities were photographed along with control embryos, using a Zeiss SteREO Discovery V8 Microscope equipped with a high-speed camera. The survival rate was determined by counting the number of dead zebrafish embryos per group at 24 h post-fertilization divided by the total number of treated embryos X 100. Danio Scope software measured the tail flicking assay (burst/min) to assess the potential neuro/muscular defect at 24 hpf. After that, the hatching percentage was calculated by counting the number of hatched embryos per group divided by the total number of treated embryos X 100 and again at 72 hpf.

4.6. Behavioral and Locomotion Assays. Three days post-fertilization, embryos were separated individually in PTUin a 96-well flat-bottomed plate and then left in an incubator for an hour to acclimatize. After acclimatization, the plate was put in the Viewpoint Zebra lab system (Noldus Information Technology, NL, USA) set at 28 °C and illuminated with white light for an adaptation period of 10 min dark, 10 min light, for 50 min. EthoVision XT 11.5 software was programmed according to the protocol needed to record individual locomotor activity. The arena settings and the detection settings were adjusted so that optimal tracking was achieved. After the experiment was carried out, the larvae were ethically euthanized. Data were exported to Excel and graphed using GraphPad Prism8.

4.7. Cardiac Toxicity: Assessment of Cardiac Function. We measured several heart function/hemodynamics parameters, including CO, blood flow, blood velocity, vessel diameter, and heartbeat, by tracking red blood cells movements in the DA and PCV from the trunk of the embryos. To do so, we used Danioscope (Noldus Information Technology Inc, USA) and MicroZebraLab blood flow from Viewpoint (version 3.4.4, Lyon, France).

At 72 h post-fertilization, we used 3% methylcellulose to fix embryos from each treated and control group, then visualized them using a Zeiss SteREO Discovery V8 Microscope equipped with a Hamamatsu Orca Flash high-speed camera and a workstation equipped with HCImage software. For each embryo, a 10 s bright field video of the beating heart and the tail was recorded at 100 frames per second (fps) and 100× magnification.

To estimate the frictional sheer stress levels in the cardiovascular system, we used blood velocity measurements. Sheer stress (τ, dynes/cm^2) was calculated using this formula $\tau = (4\,\mu V\_mean)/D$, where μ is the blood viscosity (dynes/cm^2), V is the average blood velocity (μm/s), and D is the vessel diameter (μm). Cardiac output (CO, nL/min, also known as the flow rate) was measured using this formula $F = V \times A$, where V is the average blood velocity (μm/s) and D is the vessel diameter (μm).[61]

4.8. Cardiac Failure Marker Expression. Real-time quantitative-PCR (RT-qPCR) was performed to detect the expression of *ANP/NPPA* and *BNP/NPPB*, two key heart failure markers.[62] First, RNA was isolated from whole zebrafish embryos, from both treated and control groups (20−30 each), using the IBI DNA/RNA/protein extraction kit (IBI Scientific -r IB47702, USA), according to the manufacturer's instructions. Second, we used the SuperScript IV VILO Master Mix kit (Thermo Fisher Scientific 11756050, USA), according to the manufacturer's instructions, to synthesize the first-strand cDNA. Then, quantitative analysis of specific mRNA expression was performed using TaqMan. Fast Advanced Master Mix (Applied Biosystems, USA). Specific primers and probes that were designed (Applied Biosystems, USA) against the genes of interest, atrial natriuretic peptide (*ANP/NPPA*) and brain natriuretic peptide (*BNP/NPPB*) were used in this analysis. The signal was read using RT-qPCR (QuantStudio 6 Flex RT-qPCR System). The relative quantity was calculated based on the $2^{-\Delta CT}$ method,[63] and the fold change was calculated in reference to the geomean of a group of housekeeping genes *B2M*.

4.9. Detection of Apoptotic Cells Using Acridine Orange. In this analysis, we use AO staining joined with Gen5 Microplate reader and Imager programming to measure apoptotic cells in zebrafish embryos after treatment. Embryos were placed in 10 μg/mL of AO (Sigma, St. Louis, MO) in E3 media. After 60 min of staining, embryos were washed three times in E3 media, then embryos were transferred to round-bottom 96-well plates for imaging (Corning, catalogue #4520, Corning, NY). Fluorescence was measured at the excitation wavelength of 490 nm and the emission wavelength of 520 nm. Embryos without AO staining were used to determine baseline fluorescence. The fluorescence value was expressed as relative fluorescence units (RFU 5 fluorescence reading of the experimental group minus baseline reading of the control group).

4.10. Quantitative-PCR of Apoptosis Predictive Markers. To further examine the effects of AuNRs on apoptosis markers, the mRNA expression of the apoptosis markers was measured using real-time quantitative-PCR (RT q-PCR). The total RNA of both treated and control groups was extracted, as

https://doi.org/10.1021/acsomega.2c01313
ACS Omega XXXX, XXX, XXX−XXX

described in a study by Jong *et al.*[64] The cDNA synthesis was then performed using the high-capacity cDNA Reverse Transcription Superscript IV VILO Master Mix kit (Thermo Fisher Scientific, USA), as per the manufacturer's instructions. Following the cDNA synthesis, the RT q-PCR was performed using SYBR Green PCR Master Mix (catalog number: 4309155, Applied Biosystems, USA) and specific primers (Applied Biosystems, Waltham, MA, USA) designed against the zebrafish apoptosis predictive markers genes (*P53*, *BAX/ZBAX1*, *BCL2/ZBLP2*, *CASPASE 3/ZCASPASE-3*, and *CASPASE 8/ZCASPASE-8*). The mRNA expression signal was read using RT-qPCR (QuantStudio 6 Flex RT-qPCR System), and the relative quantity calculation was carried out using the $2^{-\Delta CT}$ method, as described in a study by Rao *et al.*,[33] with the fold change being calculated in reference to the expression of the housekeeping genes *GAPDH*.

4.11. Statistical Analysis. Statistical analysis was performed using Graphpad Prism 8 software. Distribution was determined using the Kolmogorov–Smirnov normality test. Parametric data were analyzed using one-way analysis of variance (ANOVA) with the Sidak post-hoc test, two-way ANOVA with the Dunnett test, and the unpaired two-tailed *t*-test. However, nonparametric data were analyzed using the Kruskal–Wallis test with the Dunn's post-hoc test. A *p*-value of less than 0.05 was considered statistically significant.

5. CONCLUSIONS

This investigation aimed to explore the toxicity of surface-modified AuNRs toward early life stages of zebrafish due to the possible potential environmental risk posed by nanomaterials (NMs), especially with the increasing demand of these materials in various areas such as biomedicine, electronics, and catalysis. Herein, we report that high concentrations of surface-modified AuNRs show toxic effect at the early stages of normal development of the embryo. In our zebrafish model, AuNRs significantly decreased locomotion compared to control embryos, caused a decrease in all tested parameters for CO and blood flow analyses, and led to a significantly elevated expression levels of cardiac failure biomarkers, *ANP/NPPA* and *BNP/NPPB*. Moreover, our results pointed out that AuNR treatment can provoke apoptosis significantly through the *P53*, *BAX/BCL-2*, and *CASPASE* pathways at high concentrations, which indicates a harmful effect of AuNRs at the cellular level of developing zebrafish embryos. Further studies on rodents and humans are needed to confirm the toxic outcome of AuNRs.

AUTHOR INFORMATION

Corresponding Author

Maha Al-Asmakh − *Department of Biomedical Sciences, College of Health Sciences, QU Health, Qatar University, Doha 122104, Qatar; Biomedical Research Center, Qatar University, Doha 122104, Qatar*; Email: maha.alasmakh@qu.edu.qa

Authors

Zain Zaki Zakaria − *Department of Biomedical Sciences, College of Health Sciences, QU Health, Qatar University, Doha 122104, Qatar; Biomedical Research Center, Qatar University, Doha 122104, Qatar;* orcid.org/0000-0002-9656-8367

Nouf N. Mahmoud − *Department of Biomedical Sciences, College of Health Sciences, QU Health, Qatar University, Doha 122104, Qatar; Faculty of Pharmacy, Al-Zaytoonah University of Jordan, Amman 11733, Jordan;* orcid.org/0000-0002-3870-7568

Fatiha M. Benslimane − *Biomedical Research Center, Qatar University, Doha 122104, Qatar*

Huseyin C. Yalcin − *Biomedical Research Center, Qatar University, Doha 122104, Qatar*

Ala-Eddin Al Moustafa − *Biomedical Research Center and College of Medicine, QU Health, Qatar University, Doha 122104, Qatar*

Complete contact information is available at: https://pubs.acs.org/10.1021/acsomega.2c01313

Author Contributions

Conceptualization: N.M., M.A., Z.Z.Z., and A.E.M.; methodology: Z.Z.Z., N.M., and A.E.M.; software: Z.Z.Z., H.Y., and F.B; validation: N.M., A.E.M., F.B., and M.A.; formal analysis: N.M; investigation: Z.Z.Z. and N.M.; resources: H.Y., F.B., and M.A.; data curation: N.M., H.Y., F.B., and M.A.; writing—original draft preparation: N.M. and Z.Z.Z.; writing—review and editing: H.Y., N.M., M.A., and A.E.M.; visualization: Z.Z.Z.; supervision: M.A.; project administration: Z.Z.Z. and M.A.; and funding acquisition: N.M. and M.A. All authors have read and agreed to the published version of the manuscript.

Funding

This research was funded by the Qatar University–internal grant, grant number QUCP-CHS-2022-483 for M.A. and financial funding of the Deanship of Scientific Research at the Al-Zaytoonah University of Jordan (2020-2019/12/28) for N.M.

Notes

The authors declare no competing financial interest.

All experiments presented in this paper were conducted under the Qatar University's Institutional Animal Care and Use Committee (QU-IACUC) approval and Qatar University Institutional Biohazard Committee (QU-IBC), Doha.

ACKNOWLEDGMENTS

We would like to thank Dr Mohammad Ibrahim of the Central Laboratories unit at the Qatar University for his technical support. Microwave digestion and ICP–OES for the gold cellular uptake were accomplished in the Central Laboratories unit, Qatar University.

REFERENCES

(1) (a) Bayda, S.; Adeel, M.; Tuccinardi, T.; Cordani, M.; Rizzolio, F. The History of Nanoscience and Nanotechnology: From Chemical-Physical Applications to Nanomedicine. *Molecules* **2019**, *25*, 112. (b) Wang, Z. L.; Wu, W. Nanotechnology-Enabled Energy Harvesting for Self-Powered Micro-/Nanosystems. *Angew. Chem., Int. Ed.* **2012**, *51*, 11700–11721. (c) Zhang, A.; Lieber, C. M. Nano-Bioelectronics. *Chem. Rev.* **2016**, *116*, 215–257. (d) Yohan, D.; Chithrani, B. D. Applications of nanoparticles in nanomedicine. *J. Biomed. Nanotechnol.* **2014**, *10*, 2371–2392. (e) Patra, J. K.; Das, G.; Fraceto, L. F.; Campos, E. V. R.; Rodriguez-Torres, M. D. P.; Acosta-Torres, L. S.; Diaz-Torres, L. A.; Grillo, R.; Swamy, M. K.; Sharma, S.; et al. Nano based drug delivery systems: recent developments and future prospects. *J. Nanobiotechnol.* **2018**, *16*, 71.

(2) Jia, H. R.; Zhu, Y. X.; Duan, Q. Y.; Chen, Z.; Wu, F. G. Nanomaterials meet zebrafish: Toxicity evaluation and drug delivery applications. *J. Controlled Release* **2019**, *311–312*, 301–318.

(3) Johnston, H. J.; Verdon, R.; Gillies, S.; Brown, D. M.; Fernandes, T. F.; Henry, T. B.; Rossi, A. G.; Tran, L.; Tucker, C.; Tyler, C. R.; et al. Adoption of in vitro systems and zebrafish embryos as alternative models for reducing rodent use in assessments of immunological and

https://doi.org/10.1021/acsomega.2c01313
ACS Omega XXXX, XXX, XXX–XXX

oxidative stress responses to nanomaterials. *Crit. Rev. Toxicol.* **2018**, *48*, 252−271.
(4) (a) Shull, A. Y.; Hu, C.-A. A.; Teng, Y. Zebrafish as a model to evaluate peptide-related cancer therapies. *Amino Acids* **2017**, *49*, 1907−1913. (b) Haque, E.; Ward, A. C. Zebrafish as a Model to Evaluate Nanoparticle Toxicity. *Nanomaterials* **2018**, *8*, 561. (c) Yalcin, H. C. Hemodynamic studies for analyzing the teratogenic effects of drugs in the zebrafish embryo. *Teratogenicity Testing*; Springer, 2018; pp 487−495.
(5) Hill, A. J.; Teraoka, H.; Heideman, W.; Peterson, R. E. Zebrafish as a Model Vertebrate for Investigating Chemical Toxicity. *Toxicol. Sci.* **2005**, *86*, 6−19.
(6) Saleem, S.; Kannan, R. R. Zebrafish: A Promising Real-Time Model System for Nanotechnology-Mediated Neurospecific Drug Delivery. *Nanoscale Res. Lett.* **2021**, *16*, 135.
(7) Al-Thani, H. F.; Shurbaji, S.; Yalcin, H. C. Zebrafish as a Model for Anticancer Nanomedicine Studies. *Pharmaceuticals* **2021**, *14*, 625.
(8) Yen, H. J.; Horng, J. L.; Yu, C. H.; Fang, C. Y.; Yeh, Y. H.; Lin, L. Y. Toxic effects of silver and copper nanoparticles on lateral-line hair cells of zebrafish embryos. *Aquat. Toxicol.* **2019**, *215*, 105273.
(9) Duan, J.; Liang, S.; Yu, Y.; Li, Y.; Wang, L.; Wu, Z.; Chen, Y.; Miller, M. R.; Sun, Z. Inflammation-coagulation response and thrombotic effects induced by silica nanoparticles in zebrafish embryos. *Nanotoxicology* **2018**, *12*, 470−484.
(10) Hu, Q.; Wang, H.; He, C.; Jin, Y.; Fu, Z. Polystyrene nanoparticles trigger the activation of p38 MAPK and apoptosis via inducing oxidative stress in zebrafish and macrophage cells. *Environ. Pollut.* **2021**, *269*, 116075.
(11) (a) Her, S.; Jaffray, D. A.; Allen, C. Gold nanoparticles for applications in cancer radiotherapy: Mechanisms and recent advancements. *Adv. Drug Deliv. Rev.* **2017**, *109*, 84−101. (b) Bai, X.; Wang, Y.; Song, Z.; Feng, Y.; Chen, Y.; Zhang, D.; Feng, L. The Basic Properties of Gold Nanoparticles and their Applications in Tumor Diagnosis and Treatment. *Int. J. Mol. Sci.* **2020**, *21*, 2480.
(12) (a) Woźniak, A.; Malankowska, A.; Nowaczyk, G.; Grześkowiak, B. F.; Tuśnio, K.; Słomski, R.; Zaleska-Medynska, A.; Jurga, S. Size and shape-dependent cytotoxicity profile of gold nanoparticles for biomedical applications. *J. Mater. Sci. Mater. Med.* **2017**, *28*, 92. (b) Boldeiu, A.; Simion, M.; Mihalache, I.; Radoi, A.; Banu, M.; Varasteanu, P.; Nadejde, P.; Vasile, E.; Acasandrei, A.; Popescu, R. C.; et al. Comparative analysis of honey and citrate stabilized gold nanoparticles: In vitro interaction with proteins and toxicity studies. *J. Photochem. Photobiol., B* **2019**, *197*, 111519.
(13) (a) Sung, H. K.; Jo, E.; Kim, E.; Yoo, S. K.; Lee, J. W.; Kim, P. J.; Kim, Y.; Eom, I. C. Analysis of gold and silver nanoparticles internalized by zebrafish (Danio rerio) using single particle-inductively coupled plasma-mass spectrometry. *Chemosphere* **2018**, *209*, 815−822. (b) Truong, L.; Zaikova, T.; Baldock, B. L.; Balik-Meisner, M.; To, K.; Reif, D. M.; Kennedy, Z. C.; Hutchison, J. E.; Tanguay, R. L. Systematic determination of the relationship between nanoparticle core diameter and toxicity for a series of structurally analogous gold nanoparticles in zebrafish. *Nanotoxicology* **2019**, *13*, 879−893.
(14) Kim, K. T.; Zaikova, T.; Hutchison, J. E.; Tanguay, R. L. Gold nanoparticles disrupt zebrafish eye development and pigmentation. *Toxicol. Sci.* **2013**, *133*, 275−288.
(15) (a) Sanità, G.; Carrese, B.; Lamberti, A. Nanoparticle Surface Functionalization: How to Improve Biocompatibility and Cellular Internalization. *Front. Mol. Biosci.* **2020**, *7*, 587012. (b) Yang, Y.; Sunoqrot, S.; Stowell, C.; Ji, J.; Lee, C.-W.; Kim, J. W.; Khan, S. A.; Hong, S. Effect of Size, Surface Charge, and Hydrophobicity of Poly(amidoamine) Dendrimers on Their Skin Penetration. *Biomacromolecules* **2012**, *13*, 2154−2162.
(16) Shi, X.; Perry, H. L.; Wilton-Ely, J. D. E. T. Strategies for the functionalisation of gold nanorods to reduce toxicity and aid clinical translation. *Nanotheranostics* **2021**, *5*, 155−165.
(17) Mahmoud, N. N.; Alhusban, A. A.; Ali, J. I.; Al-Bakri, A. G.; Hamed, R.; Khalil, E. A. Preferential Accumulation of Phospholipid-PEG and Cholesterol-PEG Decorated Gold Nanorods into Human Skin Layers and Their Photothermal-Based Antibacterial Activity. *Sci. Rep.* **2019**, *9*, 5796.
(18) Abu-Dahab, R.; Mahmoud, N. N.; Abdallah, M.; Hamadneh, L.; Hikmat, S.; Zaza, R.; Abuarqoub, D.; Khalil, E. A. Cytotoxicity and Cellular Death Modality of Surface-Decorated Gold Nanorods against a Panel of Breast Cancer Cell Lines. *ACS Omega* **2021**, *6*, 15903−15910.
(19) Mahmoud, N. N.; Zakaria, Z. Z.; Kheraldine, H.; Gupta, I.; Vranic, S.; Al-Asmakh, M.; Al Moustafa, A.-E. The effect of surface-modified gold nanorods on the early stage of embryonic development and angiogenesis: Insight into the molecular pathways. *Int. J. Mol. Sci.* **2021**, *22*, 11036.
(20) Mahmoud, N. N.; Abu-Dahab, R.; Hamadneh, L. A.; Abuarqoub, D.; Jafar, H.; Khalil, E. A. Insights into the Cellular Uptake, Cytotoxicity, and Cellular Death Modality of Phospholipid-Coated Gold Nanorods toward Breast Cancer Cell Lines. *Mol. Pharm.* **2019**, *16*, 4149−4164.
(21) Floris, P.; Garbujo, S.; Rolla, G.; Giustra, M.; Salvioni, L.; Catelani, T.; Colombo, M.; Mantecca, P.; Fiandra, L. The Role of Polymeric Coatings for a Safe-by-Design Development of Biomedical Gold Nanoparticles Assessed in Zebrafish Embryo. *Nanomaterials* **2021**, *11*, 1004.
(22) Aubrey, B. J.; Kelly, G. L.; Janic, A.; Herold, M. J.; Strasser, A. How does p53 induce apoptosis and how does this relate to p53-mediated tumour suppression? *Cell Death Differ.* **2018**, *25*, 104−113.
(23) Storer, N. Y.; Zon, L. I. Zebrafish models of p53 functions. *Cold Spring Harbor Perspect. Biol.* **2010**, *2*, a001123.
(24) Xiang, H.; Kinoshita, Y.; Knudson, C. M.; Korsmeyer, S. J.; Schwartzkroin, P. A.; Morrison, R. S. Bax involvement in p53-mediated neuronal cell death. *J. Neurosci.* **1998**, *18*, 1363−1373.
(25) Tzifi, F.; Economopoulou, C.; Gourgiotis, D.; Ardavanis, A.; Papageorgiou, S.; Scorilas, A. The role of BCL2 family of apoptosis regulator proteins in acute and chronic leukemias. *Adv. Hematol.* **2012**, *2012*, 524308.
(26) Shalini, S.; Dorstyn, L.; Dawar, S.; Kumar, S. Old, new and emerging functions of caspases. *Cell Death Differ.* **2015**, *22*, 526−539.
(27) Alkilany, A. M.; Thompson, L. B.; Boulos, S. P.; Sisco, P. N.; Murphy, C. J. Gold nanorods: their potential for photothermal therapeutics and drug delivery, tempered by the complexity of their biological interactions. *Adv. Drug Deliv. Rev.* **2012**, *64*, 190−199.
(28) Zhang, J.; Mou, L.; Jiang, X. Surface chemistry of gold nanoparticles for health-related applications. *Chem. Sci.* **2020**, *11*, 923−936.
(29) Zhang, B.; Chen, J.; Cao, Y.; Chai, O. J. H.; Xie, J. Ligand Design in Ligand-Protected Gold Nanoclusters. *Small* **2021**, *17*, 2004381.
(30) Zhang, Y.; Xu, D.; Li, W.; Yu, J.; Chen, Y. Effect of Size, Shape, and Surface Modification on Cytotoxicity of Gold Nanoparticles to Human HEp-2 and Canine MDCK Cells. *J. Nanomater.* **2012**, *2012*, 1.
(31) Wang, Z.; Xie, D.; Liu, H.; Bao, Z.; Wang, Y. Toxicity assessment of precise engineered gold nanoparticles with different shapes in zebrafish embryos. *RSC Adv.* **2016**, *6*, 33009−33013.
(32) Sabella, S.; Galeone, A.; Vecchio, G.; Cingolani, R.; Pompa, P. AuNPs are toxic in vitro and in vivo: a review. *J. Nanosci. Lett.* **2011**, *1*, 145−165.
(33) Browning, L. M.; Lee, K. J.; Huang, T.; Nallathamby, P. D.; Lowman, J. E.; Nancy Xu, X.-H. N. Random walk of single gold nanoparticles in zebrafish embryos leading to stochastic toxic effects on embryonic developments. *Nanoscale* **2009**, *1*, 138−152.
(34) Browning, L. M.; Huang, T.; Xu, X.-H. N. Real-time in vivo imaging of size-dependent transport and toxicity of gold nanoparticles in zebrafish embryos using single nanoparticle plasmonic spectroscopy. *Interface Focus* **2013**, *3*, 20120098.
(35) (a) Abdelrasoul, G. N.; Magrassi, R.; Dante, S.; d'Amora, M.; d'Abbusco, M. S.; Pellegrino, T.; Diaspro, A. PEGylated gold nanorods as optical trackers for biomedical applications: an in vivo and in vitro comparative study. *Nanotechnology* **2016**, *27*, 255101. (b) Fu, L.-H.; Yang, J.; Zhu, J.-F.; Ma, M.-G. Synthesis of gold nanoparticles and their applications in drug delivery. *Metal Nanoparticles in Pharma*; Springer, 2017; pp 155−191

https://doi.org/10.1021/acsomega.2c01313
ACS Omega XXXX, XXX, XXX−XXX

(36) Mesquita, B. S. M. *Acute and Developmental Toxicity of Gold Nanorods on Zebrafish (Danio rerio) Embryos*, 2016.
(37) Galindo, T. P. S. *Nanomaterials: A Brief Review About the Influence of Environmental Factors on their Ecotoxicity to Biota*.
(38) Galindo, T.; Pereira, R.; Freitas, A.; Santos-Rocha, T.; Rasteiro, M.; Antunes, F.; Rodrigues, D.; Soares, A.; Gonçalves, F.; Duarte, A.; Lopes, I. Toxicity of organic and inorganic nanoparticles to four species of white-rot fungi. *Sci. Total Environ.* **2013**, *458*−*460*, 290−297.
(39) (a) Seidelmann, S. B.; Vardeny, O.; Claggett, B.; Yu, B.; Shah, A. M.; Ballantyne, C. M.; Selvin, E.; MacRae, C. A.; Boerwinkle, E.; Solomon, S. D. An NPPB promoter polymorphism associated with elevated N-terminal pro−B-type natriuretic peptide and lower blood pressure, hypertension, and mortality. *J. Am. Heart Assoc.* **2017**, *6*, No. e005257. (b) Goetze, J. P.; Bruneau, B. G.; Ramos, H. R.; Ogawa, T.; de Bold, M. K.; de Bold, J. Cardiac natriuretic peptides. *Nat. Rev. Cardiol.* **2020**, *17*, 698−717.
(40) Albert, I. *Zebrafish as a Model System for Safety Pharmacology, using a Glucocorticoid and an Antimicrobial Peptide as Test Substances*; Universitetet i Tromsø, 2013.
(41) Yabu, T.; Kishi, S.; Okazaki, T.; Yamashita, M. Characterization of zebrafish caspase-3 and induction of apoptosis through ceramide generation in fish fathead minnow tailbud cells and zebrafish embryo. *Biochem. J.* **2001**, *360*, 39−47.
(42) Eimon, P. M. Studying apoptosis in the Zebrafish. *Methods Enzymol.* **2014**, *544*, 395−431.
(43) Selim, M. E.; Hendi, A. A. Gold nanoparticles induce apoptosis in MCF-7 human breast cancer cells. *Asian Pac. J. Cancer Prev.* **2012**, *13*, 1617−1620.
(44) Eimon, P. M.; Kratz, E.; Varfolomeev, E.; Hymowitz, S. G.; Stern, H.; Zha, J.; Ashkenazi, A. Delineation of the cell-extrinsic apoptosis pathway in the zebrafish. *Cell Death Differ.* **2006**, *13*, 1619−1630.
(45) (a) Lanvin, O.; Gouilleux, F.; Mullié, C.; Mazière, C.; Fuentes, V.; Bissac, E.; Dantin, F.; Mazière, J.-C.; Régnier, A.; Lassoued, K.; Gouilleux-Gruart, V. Interleukin-7 induces apoptosis of 697 pre-B cells expressing dominant-negative forms of STAT5: evidence for caspase-dependent and-independent mechanisms. *Oncogene* **2004**, *23*, 3040−3047. (b) Youle, R. J.; Strasser, A. The BCL-2 protein family: opposing activities that mediate cell death. *Nat. Rev. Mol. Cell Biol.* **2008**, *9*, 47−59. (c) Hsieh, Y.-C.; Chang, M.-S.; Chen, J.-Y.; Jong-Young Yen, J. J.-Y.; Lu, I.-C.; Chou, C.-M.; Huang, C.-J. Cloning of zebrafish BAD, a BH3-only proapoptotic protein, whose overexpression leads to apoptosis in COS-1 cells and zebrafish embryos. *Biochem. Biophys. Res. Commun.* **2003**, *304*, 667−675. (d) Hughes, P.; Bouillet, P.; Strasser, A. Role of Bim and other Bcl-2 family members in autoimmune and degenerative diseases. *Apoptosis and Its Relevance to Autoimmunity* **2006**, *9*, 74−94. (e) Arnaud, E.; Ferri, K.; Thibaut, J.; Haftek-Terreau, Z.; Aouacheria, A.; Le Guellec, D.; Lorca, T.; Gillet, G. The zebrafish bcl-2 homologue Nrz controls development during somitogenesis and gastrulation via apoptosis-dependent and-independent mechanisms. *Cell Death Differ.* **2006**, *13*, 1128−1137.
(46) (a) Asharani, P.; lianwu, Y.; Gong, Z.; Valiyaveettil, S. Comparison of the toxicity of silver, gold and platinum nanoparticles in developing zebrafish embryos. *Nanotoxicology* **2011**, *5*, 43−54. (b) Mesquita, B.; Lopes, I.; Silva, S.; Bessa, M. J.; Starykevich, M.; Carneiro, J.; Galvão, T. L.; Ferreira, M. G.; Tedim, J.; Teixeira, J. P. Gold nanorods induce early embryonic developmental delay and lethality in zebrafish (Danio rerio). *J. Toxicol. Environ. Health, Part A* **2017**, *80*, 672−687.
(47) (a) van Pomeren, M.; Peijnenburg, W.; Vlieg, R.; van Noort, S.; Vijver, M. The biodistribution and immuno-responses of differently shaped non-modified gold particles in zebrafish embryos. *Nanotoxicology* **2019**, *13*, 558−571. (b) Ganeshkumar, M.; Sastry, T. P.; Sathish Kumar, M. S.; Dinesh, M. G.; Kannappan, S.; Suguna, L. Sun light mediated synthesis of gold nanoparticles as carrier for 6-mercaptopurine: Preparation, characterization and toxicity studies in zebrafish embryo model. *Mater. Res. Bull.* **2012**, *47*, 2113−2119.
(48) d'Amora, M.; Raffa, V.; De Angelis, F.; Tantussi, F. Toxicological Profile of Plasmonic Nanoparticles in Zebrafish Model. *Int. J. Mol. Sci.* **2021**, *22*, 6372.
(49) Yang, L.; Kuang, H.; Zhang, W.; Aguilar, Z. P.; Wei, H.; Xu, H. Comparisons of the biodistribution and toxicological examinations after repeated intravenous administration of silver and gold nanoparticles in mice. *Sci. Rep.* **2017**, *7*, 3303.
(50) Rambanapasi, C.; Zeevaart, J. R.; Buntting, H.; Bester, C.; Kotze, D.; Hayeshi, R.; Grobler, A. Bioaccumulation and subchronic toxicity of 14 nm gold nanoparticles in rats. *Molecules* **2016**, *21*, 763.
(51) (a) Elci, S. G.; Jiang, Y.; Yan, B.; Kim, S. T.; Saha, K.; Moyano, D. F.; Yesilbag Tonga, G.; Jackson, L. C.; Rotello, V. M.; Vachet, R. W. Surface charge controls the suborgan biodistributions of gold nanoparticles. *ACS Nano* **2016**, *10*, 5536−5542. (b) Chanda, N.; Kattumuri, V.; Shukla, R.; Zambre, A.; Katti, K.; Upendran, A.; Kulkarni, R. R.; Kan, P.; Fent, G. M.; Casteel, S. W.; Smith, C. J.; Boote, E.; Robertson, J. D.; Cutler, C.; Lever, J. R.; Katti, K. V.; Kannan, R. Bombesin functionalized gold nanoparticles show in vitro and in vivo cancer receptor specificity. *Proc. Natl. Acad. Sci. U.S.A.* **2010**, *107*, 8760−8765.
(52) (a) Sani, A.; Cao, C.; Cui, D. Toxicity of gold nanoparticles (AuNPs): A review. *Biochem. Biophys. Rep.* **2021**, *26*, 100991. (b) Enea, M.; Pereira, E.; Peixoto de Almeida, M.; Araújo, A. M.; Bastos, M. d. L.; Carmo, H. Gold nanoparticles induce oxidative stress and apoptosis in human kidney cells. *Nanomaterials* **2020**, *10*, 995.
(53) Ramachandran, R.; Krishnaraj, C.; Kumar, V.; Harper, S. L.; Kalaichelvan, T. P.; Yun, S.-I. In vivo toxicity evaluation of biologically synthesized silver nanoparticles and gold nanoparticles on adult zebrafish: a comparative study. *3 Biotech* **2018**, *8*, 1−12.
(54) Jawaid, P.; Rehman, M. U.; Zhao, Q.-L.; Misawa, M.; Ishikawa, K.; Hori, M.; Shimizu, T.; Saitoh, J.-i.; Noguchi, K.; Kondo, T. Small size gold nanoparticles enhance apoptosis-induced by cold atmospheric plasma via depletion of intracellular GSH and modification of oxidative stress. *Cell Death Discovery* **2020**, *6*, 83.
(55) (a) Chakraborty, C.; Sharma, A. R.; Sharma, G.; Lee, S.-S. Zebrafish: A complete animal model to enumerate the nanoparticle toxicity. *J. Nanobiotechnol.* **2016**, *14*, 65. (b) Li, X.; Hu, Z.; Ma, J.; Wang, X.; Zhang, Y.; Wang, W.; Yuan, Z. Yuan, Z. The systematic evaluation of size-dependent toxicity and multi-time biodistribution of gold nanoparticles. *Colloids Surf., B* **2018**, *167*, 260−266.
(56) Cho, W.-S.; Cho, M.; Jeong, J.; Choi, M.; Cho, H.-Y.; Han, B. S.; Kim, S. H.; Kim, H. O.; Lim, Y. T.; Chung, B. H.; Jeong, J. Acute toxicity and pharmacokinetics of 13 nm-sized PEG-coated gold nanoparticles. *Toxicol. Appl. Pharmacol.* **2009**, *236*, 16−24.
(57) (a) Ali, G. E.; Ibrahim, M. A.; El-Deeb, A. H.; Amer, H.; Zaki, S. M. Pulmonary deregulation of expression of miR-155 and two of its putative target genes; PROS1 and TP53INP1 associated with gold nanoparticles (AuNPs) administration in rat. *Int. J. Nanomed.* **2019**, *14*, 5569. (b) Yang, Y.; Fan, S.; Chen, Q.; Lu, Y.; Zhu, Y.; Chen, X.; Xia, L.; Huang, Q.; Zheng, J.; Liu, X. Acute exposure to gold nanoparticles aggravates lipopolysaccharide-induced liver injury by amplifying apoptosis via ROS-mediated macrophage-hepatocyte crosstalk. *Journal of Nanobiotechnology* **2022**, *20*, 37.
(58) Untergasser, G.; Rumpold, H.; Plas, E.; Madersbacher, S.; Berger, P. A low-molecular-weight fraction of human seminalplasma activates adenylyl cyclase and induces caspase3-independent apoptosis in prostatic epithelial cellsby decreasing mitochondrial potential andBcl-2/Bax ratio. *FASEB J.* **2001**, *15*, 673.
(59) Ding, F.; Li, Y.; Liu, J.; Liu, L.; Yu, W.; Wang, Z.; Ni, H.; Liu, B.; Chen, P. Overendocytosis of gold nanoparticles increases autophagy and apoptosis in hypoxic human renal proximal tubular cells. *Int. J. Nanomed.* **2014**, *9*, 4317.
(60) Westerfield, M. *The Zebrafish Book: a Guide for the Laboratory use of Zebrafish*. http://zfin. org/zf_info/zfbook/zfbk. html, 2000.
(61) (a) Zakaria, Z. Z.; Benslimane, F. M.; Nasrallah, G. K.; Shurbaji, S.; Younes, N. N.; Mraiche, F.; Da'as, S. I.; Yalcin, H. C. J. B. R. I. Using Zebrafish for Investigating the Molecular Mechanisms of Drug-Induced Cardiotoxicity. *Biomed Res Int.* **2018**, *2018*, 1642684. (b) Yalcin, H.; Abuhabib, U.; Kitaz, N.; Mohamed, A.; Zakaria, Z. Generating an imagingbased approach for enhanced structural and functional analysis of zebrafish cardiovascular systems. *Qatar Foundation Annual Research*

https://doi.org/10.1021/acsomega.2c01313
ACS Omega XXXX, XXX, XXX−XXX

Conference Proceedings, 2018; HBKU Press Qatar; Vol. *2018*, p HBPD769.

(62) (a) Becker, J. R.; Chatterjee, S.; Robinson, T. Y.; Bennett, J. S.; Panáková, D.; Galindo, C. L.; Zhong, L.; Shin, J. T.; Coy, S. M.; Kelly, A. E.; Roden, D. M.; Lim, C. C.; MacRae, C. A. Differential activation of natriuretic peptide receptors modulates cardiomyocyte proliferation during development. *Development* **2014**, *141*, 335−345. (b) Becker, J. R.; Robinson, T. Y.; Sachidanandan, C.; Kelly, A. E.; Coy, S.; Peterson, R. T.; MacRae, C. A. In vivo natriuretic peptide reporter assay identifies chemical modifiers of hypertrophic cardiomyopathy signalling. *Cardiovascular research* **2012**, *93*, 463−470. (c) Narumanchi, S.; Wang, H.; Perttunen, S.; Tikkanen, I.; Lakkisto, P.; Paavola, J. Zebrafish Heart Failure Models. *Front. Cell Dev. Biol.* **2021**, *9*, 662583.

(63) Rao, X.; Huang, X.; Zhou, Z.; Lin, X. An improvement of the 2^(-delta delta CT) method for quantitative real-time polymerase chain reaction data analysis. *Biostat. Bioinforma. Biomath.* **2013**, *3* (3), 71−85.

(64) de Jong, M.; Rauwerda, H.; Bruning, O.; Verkooijen, J.; Spaink, H. P; Breit, T. M RNA isolation method for single embryo transcriptome analysis in zebrafish. *BMC Res Notes* **2010**, *3*, 73.

https://doi.org/10.1021/acsomega.2c01313
ACS Omega XXXX, XXX, XXX−XXX